IEEE Access
The journal for rapid open access publishing

IEEE Xplore Digital Library
http://ieeexplore.ieee.org/Xplore

Dynamic Resource Allocation for Optimized Latency and Reliability in Vehicular Networks

Muhammad Ikram Ashraf, *Student Member, IEEE,*
Chen-Feng Liu, *Student Member, IEEE,*
Mehdi Bennis, *Senior Member, IEEE,* Walid Saad, *Senior Member, IEEE,* and
Choong Seon Hong, *Senior Member, IEEE*

***Abstract*—Supporting ultra-reliable and low-latency communications (URLLC) is key for vehicular traffic safety and other mission-critical applications. In this paper, a novel proximity and quality-of-service (QoS)-aware resource allocation framework for vehicle-to-vehicle (V2V) communication is proposed. The proposed approach exploits the spatial and temporal traffic characteristics of the vehicles. The proposed scheme incorporates physical proximity and traffic demands of vehicles so as to minimize the total network cost which captures the total transmission power and queuing latency under reliability constraints. This problem is formulated as a power minimization problem for which a Lyapunov framework is used to decompose the problem into two interrelated sub-problems of resource block (RB) allocation and power optimization (RAPO). To minimize the overhead introduced by frequent information exchange between vehicles and the roadside unit (RSU), we further decomposed the resource allocation problem into two interrelated subproblems. First, a novel RSU-assisted virtual clustering mechanism is proposed to group vehicles into disjoint zones based on mutual interference. Second, a per-zone matching game is proposed to allocate resources blocks (RBs) to each vehicle user equipment (VUE) based on vehicles's traffic demands and their latency and reliability requirements. The problem is cast as a one-to-many matching game in which VUEs pairs and RBs rank one another using preference relations that capture both the queue dynamics and interference. To solve this game, a semi-decentralized algorithm is proposed in which VUEs and RBs reach a stable matching. Subsequently, a power minimization solution is proposed for each VUE pair over the assigned subset of RBs. Simulation results for a Manhattan model show that the proposed scheme outperforms a state-of-art baseline and reaches up to 45% reduction in the queuing latency and 94% improvement in reliability.**

***Index Terms*—5G, Lyapunov optimization, matching theory, power optimization, ultra-reliable low latency communications (URLLC)**

I. Introduction

Vehicular communication is emerging as a promising enabler for intelligent transportation systems (ITSs). In modern vehicle-to-vehicle (V2V) applications, e.g., automatic braking, safety concerns and lane change alerts, still pose substantial challenges for vehicular networks [1]. These applications typically require efficient proximity-aware cooperative among by exchanging safety messages among vehicles to reduce the risk of traffic accidents. ETSI has standardized two types of safety messages: decentralized environmental notification message (DENM) and cooperative awareness message (CAM) [2], [3]. In order to exchange these messages, ultra-reliability and low-latency communications (URLLC) is critical [4]. URLCC applications with closed-loop control, such as vehicle collision avoidance, end-to-end or round-trip latency requirement is around 1 ms while the overall packet loss probability is below 99.999% for small packet sizes, e.g., 20 bytes or even smaller [5]–[7]. 5G specifies a queuing latency of 0.125 ms in order to satisfy 1 ms end-to-end latency bound [8]. To this end, URLLC requirements become essential part of the next generation vehicular networks.

Efficient radio resource management (RRM) techniques are essential to satisfy the stringent URLLC quality-of-service (QoS) requirements. Dynamic and flexible RRM techniques in V2V networks offer the possibility to adapt to the localized service requirements and, hence, need to be carefully designed. Legacy solutions for V2V communication rely on ad hoc communication over the IEEE 802.11p standard and backend-based communication over the long term evolution (LTE) cellular standard [9]. Nevertheless, due to a dynamic nature of vehicular communication, legacy solutions suffer from several drawbacks such as network scalability, efficient resource management, unbounded delay, lack of reliability guarantees, and varying QoS requirements [1], [10], [11]. On the other hand, the performance of the LTE system for vehicular communication is always unsatisfactory, particularly for URLLC scenarios [4], [11]. Therefore, seeking optimal RRM solutions to enable V2V communication are strongly desirable.

A. Related Work

RRM has a significant impact on the performance of vehicular networks. A vehicular network RRM mechanism must be carefully designed with particular attention to interference

This research was supported in part by the U.S. National Science Foundation under Grants CNS-1513697 and AST-1506297.

M. I. Ashraf was with the Centre for Wireless Communications, University of Oulu, Oulu 90014, Finland and currently with Ericsson, Research Finland (e-mail: ikram.ashraf@oulu.fi).

C.-F. Liu is with the Centre for Wireless Communications, University of Oulu, Oulu 90014, Finland (e-mail: chen-feng.liu@oulu.fi).

M. Bennis is with the Centre for Wireless Communications, University of Oulu, Oulu 90014, Finland and Kyung Hee University, South Korea (e-mail: mehdi.bennis@oulu.fi).

W. Saad is with Wireless@VT, Bradley Department of Electrical and Computer Engineering, Virginia Tech, Blacksburg, VA 24061 USA (e-mail: walids@vt.edu).

C. S. Hong is with the Department of Computer Engineering, Kyung Hee University, South Korea (e-mail: cshong@khu.ac.kr).

Digital Object Identifier: 10.1109/ACCESS.2018.2876548

Table I: Summary of resource allocation techniques in the existing V2V literature.

Reference	RB allocation	Latency & reliability	Power allocation	Queue dynamics
[9]	IEEE 802.11p CSMA/CA	×	✓	×
[11]	Centralized solution + orthogonal RB allocation	✓	✓	×
[12]	Centralized heuristic solution	×	×	×
[13]	Heuristic solution	✓	×	×
[14]	Distributed solution	✓	×	×
[15]	Centralized scheme	Limited	✓	×
[16]	Hybrid solution	×	×	×
[17]	Distributed solution	×	×	×
[18]	Distributed solution	×	✓	×
[19]	Centralized scheme	×	×	×
[20]	Semi-distributed scheme (PF)	×	×	×

mitigation due to resource reuse while satisfying stringent URLLC requirements [6], [21]. In particular, the high mobility of vehicles brings challenges in channel quality acquisition. Problems pertaining to RRM and network modeling with URLLC metrics have been recently studied for many types of networks including vehicular and device-to-device networks [11]–[24].

In [11] the authors proposed a centralized heuristic QoS-based RRM scheme by solving sum-rate maximization problem but without considering for the traffic queue state information (QSI) at vehicles. A heuristic location-dependent resource allocation for V2V is proposed in [12], where orthogonal resource blocks (RBs) are allocated to different geographical areas. However, the work in [12] relies on a full buffer traffic model which can lead to severe queuing latency. A resource sharing algorithm while incorporate matrix spectral radius to bound the accumulated interference is proposed in [13]. The objective of RRM algorithm in [13] is to maximizes the number of concurrent V2V transmissions while ensuring reliability constraints. In [14], a low-complexity outage-optimal distributed channel allocation scheme is proposed based on a bipartite matching formulation for V2V links. The work in [15] proposed a spectrum sharing and power allocation scheme subject to the outage probability based on signal-to-interference-plus-noise ratio (SINR).

Additionally, in [16] authors use dynamic programming to search for an optimal clustering solution that minimizes the number of resources consumed by vehicular ad hoc networks (VANETs). In [17], a distributed resource allocation approach is presented by exploring the spatio-temporal aspects (in terms of load and vehicles' physical proximity) of V2V networks to minimize the total network cost which captures the tradeoffs between load (i.e., service delay) and successful transmissions. The authors in [18] proposed a geo-location based resource reuse and user selection approach in which two different distributed power control schemes are introduced for various applications in vehicular networks. A centralized resource allocation scheme based on vehicle locations is presented in [19]. In our previous work [20], we studied the problem of power optimization in V2V communication considering latency and reliability aspects. However, this work differs significantly from [20] in many folds: i) We group VUEs into dynamic zones instead of a fixed number of zones, leveraging the spatial and temporal nature of V2V communication, ii) We propose a novel algorithm based on matching theory for dynamic allocation of RBs to VUEs inside each zone, whereas [20] assumes proportional fair (PF) allocation of RBs, iii) Contrary to [20], we propose an interference estimation based on the history of VUEs traffic demand and their geographical information. Furthermore, we examine the latency and reliability constraints to analyze the queue dynamics in more details as discussed in Section II.

Moreover, a performance analysis framework is proposed for optimizing a platoon's operation while jointly taking into account the delay of the V2V network and the stability of the vehicle's control system [24]. However, the works in [16]–[19] fail to take into account the stringent latency and reliability requirements. Meanwhile, the work in [24] assumes resource allocation to be pre-determined, rather than optimized. The state-of-the-art contributions in the resource allocation of V2V communication is summarized in Table I.

B. Motivations and Contributions

Although interestingly, none of the aforementioned works consider the stochastic nature of traffic arrival and data queue dynamics while satisfying stringent URLLC requirements [11]–[19]. Meanwhile, the majority of existing V2V works [11]–[19] assume that full global channel state information (CSI) is available at all network entities, which is impractical for vehicular networks. Due to the fast-varying channel conditions and topological environments, frequent exchange of local information and control signaling can incur tremendous overhead and leads to a degradation in the network performance [9], [11], [19].

Motivated by the above shortcomings, the main contribution of this work is a fresh start architecture for latency and reliability-aware resource allocation for V2V communications. Unlike existing works, our proposed approach considers RBs allocation and power control jointly such that the interference is minimized while taking into account both the geographical information and the queue dynamics. To capture the dynamic traffic demands, each vehicle user equipment (VUE) is assumed to be equipped with a traffic queue buffer to store the stochastic data arrivals. For better resource utilization and to reduce queuing latency and maximum reliability, we exploit QSI together with the conventional physical layer metrics.

We propose a Lyapunov based stochastic optimization framework [25] to jointly optimize resource allocation and power allocation while satisfying the queuing latency and reliability requirements. The problem is formulated as a network power minimization wherein the main objective is to minimize the Lyapunov drift-plus-penalty function that captures the trade-off between the transmit power and stability of the system queues. Due to the dynamic nature (e.g., CSI, QSI, network topology, etc.) of V2V networks, performing dynamic resource allocation requires the knowledge of the entire network state information which incurs significant overhead. Therefore, the main optimization problem is decomposed into two interrelated subproblems that are solved in a semi-distributed fashion at the roadside unit (RSU) and VUE level.

First, by exploiting the spatial-temporal information of vehicles, the RSU groups vehicle pairs into a number of zones based on their location and traffic patterns. Then, in order to allocate RBs to each VUE pair, we formulate a per-zone one-to-many matching game in which VUEs and RBs are the players, which rank one another based on a set of preferences that account for interference, QSI and traffic demands. The aim of the matching game is to find a suitable and stable allocation between VUEs and RBs. Furthermore, the goal of the matching game is to associate the VUEs to a feasible set of RBs while satisfying latency and reliability constraints. To solve this game, we propose a distributed algorithm that is guaranteed to converge to a two-sided stable and Pareto optimal matching between VUEs and RBs. Subsequently, once the stable and optimal RB allocation solution is found, every VUE optimizes its transmit power over allocated RBs while satisfying latency and reliability constraints. Simulation results validate the effectiveness and performance of the proposed approach as compared to a baseline in terms of latency and reliability. The results show 94% improvement in reliability and 45% reduction in queuing latency as compared to baseline.

The rest of this paper is organized as follows. Section II describes the system model and presents the optimization problem. The optimization problem is further simplified using the Lyapunov framework and a semi-distributed approach is presented in Section III. Following the semi-distributed approach, a novel zone formation mechanism is detailed in Section IV. Section V discusses the proposed matching algorithm and power allocation scheme. The performance of the proposed framework is analyzed in Section VI. Finally, Section VII concludes the paper. The notations used throughout this paper are listed in Table II.

Table II: Summary of Notations

Notation	Definition
$\mathcal{K}$	Set of VUE pairs
$\mathcal{N}$	Set of RBs
ω	Bandwidth of an RB
t	Time slot index
$x_{kn}(t)$	RB usage indicator in time slot t
$\lambda_k(t)$	Traffic arrival at VUE k in slot t
$q_k(t)$	Physical queue value at VUE k in slot t
$f_k(t)$	Virtual queue value at VUE k in slot t
$j_k(t)$	Virtual queue value at VUE k in slot t
$R_{kn}(t)$	Transmission rate of VUE k over RB n in slot t
$p_{kn}(t)$	Transmit power of VUE k over RB n in slot t
$h_{kk'n}(t)$	Wireless channel from VUE k to VUE k' over RB n in slot t
σ^2	Noise variance
L_k	Maximum allowed queue length at VUE k
ϵ_k	Tunable tolerance parameter for VUE k
$\mathcal{Z}$	Set of zones
$\mathcal{K}_z$	Set of VUE pairs in zone z
$\mathcal{N}_k$	Set of RBs allocated to VUE k
$\boldsymbol{s}_k$	Geographical coordinates of VUE k
$s_{kk'}$	Gaussian distance similarity between VUE k and k'
$c_{kk'}$	Gaussian traffic arrival dissimilarity between VUE k and k'
v	Control parameter
$U_{kn}(t)$	Utility of VUE k over RB n at slot t
$U_n(t)$	Utility of RB n at slot t
$\succ$	Preference relation
$\mathbb{E}[\cdot]$	Expectation operator
$\Pr(\cdot)$	Probability measurement
$\mathbb{1}\{\cdot\}$	Indicator function

II. System Model and Problem Formulation

A. Network and Traffic Model

We consider a V2V network following the Manhattan mobility model as illustrated in Fig. 1. The V2V network is composed of a single RSU covering set $\mathcal{K}$ of K VUE transmitter-receiver (Tx-Rx) pairs. During the entir communication period, it is assumed that the VUE pair configuration is fixed. In order to model the vehicular mobility, a safety distance is incorporated between Tx-Rx of a single VUE pair. The safety distance is bounded and smaller compared to the considered network area. In this work, the available resources are represented in both frequency and time domains, where the whole bandwidth is divided into set of $\mathcal{N}$ RBs as shown in Fig. 1. Additionally, $|h_{kk'n}(t)|^2$ denotes the channel gain of a VUE transmitter of pair k to the VUE receiver of pair k' over RB n in time slot t. We define $x_{kn}(t)$ as the indicator variable indicating that VUE k uses RB n at time slot t. To transmit information to its VUE receiver, the transmitter of pair k allocates power $p_{kn}(t)$ over RB n in time slot t with $\sum_{n\in\mathcal{N}} x_{kn}(t)p_{kn}(t) \leq P_k^{\max}$ where $P_k^{\max}$ is VUE pair k's total power budget. Thus, the data rate of VUE pair k in time slot t is:

$$R_{kn}(t) = \omega \log_2\left(1 + \frac{x_{kn}(t)p_{kn}(t)|h_{kkn}(t)|^2}{\sigma^2 + I_{kn}(t)}\right), \quad (1)$$

$$R_k(t) = \sum_{n\in\mathcal{N}} R_{kn}(t), \quad (2)$$

where ω represents the bandwidth of an RB and σ^2 is the variance of the additive white Gaussian noise. The interference term $I_{kn}(t)$ in (1) represents the aggregate interference at VUE k caused by the transmission of other VUEs $k' \in \mathcal{K}$ on the same RB n, and is given by:

$$I_{kn}(t) = \sum_{k'\in\mathcal{K}\setminus k} x_{kn}(t)p_{k'n}(t)|h_{k'kn}(t)|^2. \quad (3)$$

Moreover, each VUE transmitter has a queue buffer to store data for its VUE receiver. Let $\boldsymbol{q}(t) = [q_1(t), \ldots, q_K(t)]$ be the traffic queue length vector in time slot t where $q_k(t)$ denotes the queue length of a given VUE pair $k \in \mathcal{K}$. The evolution

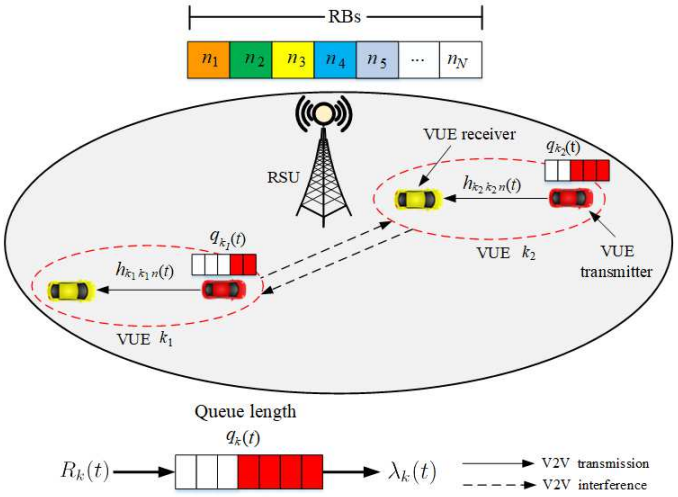

Figure 1: Interference between different VUE pairs k_1 and k_2 using the same set of RBs $n \in \mathcal{N}$

of $q_k(t)$ is given by:

$$q_k(t+1) = \left[q_k(t) - \tau R_k(t)\right]^+ + \lambda_k(t), \tag{4}$$

where, τ is the time slot duration while $\lambda_k(t)$, with $\bar{\lambda}_k = \mathbb{E}[\lambda_k(t)]$, is the traffic arrival at the transmitter of pair k in time slot t. Here $[\cdot]^+ = \max\{\cdot, 0\}$ indicates that the amount of served data cannot exceed the amount of the stored data in the queue. Without loss of generality, we assume $q_k(1) = 0, \forall\, k \in \mathcal{K}$, as the initial queue length.

B. Problem Formulation

Our objective is to find an efficient RB allocation and power optimization (RAPO) solution while meeting the latency and reliability requirements [8]. In our considered V2V scenario, the latency is defined as the *queuing latency*, defined as the time a packet waits in a queue until it can be successfully transmitted to the VUE receiver. According to Little's law [26], the average queuing latency at VUE pair k is proportional to $\bar{q}_k/\bar{\lambda}_k$, where $\bar{q}_k = \lim_{T\to\infty} \frac{1}{T}\sum_{t=1}^{T} \mathbb{E}[q_k(t)]$ is the time averaged expected queue length. Thus, we impose an upper bound d_k on the average queuing latency of each VUE pair k, as follow:

$$\frac{\bar{q}_k}{\bar{\lambda}_k} \leq d_k, \ \forall\, k \in \mathcal{K}. \tag{5}$$

In addition to queuing latency, the queue length is also related to the reliability requirements for V2V communication. We further note that the delay (or queue length) bound violation is related to reliability. Thus, taking into account the latency and reliability requirements, we characterize the delay bound violation with a tolerable probability. In particular, a probabilistic constraint is imposed on the queue length of each VUE pair k, i.e.,

$$\lim_{T\to\infty} \frac{1}{T} \sum_{t=1}^{T} \Pr\left(q_k(t) \geq L_k\right) \leq \epsilon_k, \ \forall\, k \in \mathcal{K}, \tag{6}$$

where L_k and $\epsilon_k \ll 1$ are the allowable queue length and tolerable violation probability, respectively. Without loss of generality, we replace the non-linear constraint in (6) with linear equivalents to render the probabilistic constrain tractable as:

$$\lim_{T\to\infty} \frac{1}{T} \sum_{t=1}^{T} \mathbb{E}\big[\mathbb{1}\{q_k(t) \geq L_k\}\big] \leq \epsilon_k. \tag{7}$$

In order to increase the reliability and reduce latency, a large number of data packets needs to be sent within the given latency bound. However, this might over-allocate resources (i.e., RB, transmit power) to a given VUE. Typically, the transmit power in successive slots is coupled with the resource allocation and queue dynamics (i.e., queue length). Therefore, the transmission power can better capture the real-world performance of a vehicular network while minimizing the queuing latency and improving reliability. The RSU's objective is to find an optimal RB allocation and power allocation policy which minimizes the network transmission power while satisfying (5) and (7). Let $\boldsymbol{X}(t) = [x_{kn}(t)]$ be the RB allocation matrix and $\boldsymbol{P}(t) = [p_{kn}(t)]$ be the power matrix in time slot t. Therefore, we pose the following joint resource allocation and power allocation optimization problem whose goal is to minimize time-average power:

$$\underset{X(t),P(t)}{\text{minimize}} \quad \sum_{k\in\mathcal{K}} \sum_{n\in\mathcal{N}} \bar{p}_{kn} \tag{8a}$$

$$\text{subject to} \quad \lim_{T\to\infty} \frac{1}{T} \sum_{t=1}^{T} \mathbb{E}[q_k(t)] \leq \bar{\lambda}_k d_k, \ \forall\, k \in \mathcal{K}, \tag{8b}$$

$$\lim_{T\to\infty} \frac{1}{T} \sum_{t=1}^{T} \mathbb{E}\big[\mathbb{1}\{q_k(t) \geq L_k\}\big] \leq \epsilon_k, \ \forall\, k \in \mathcal{K}, \tag{8c}$$

$$\sum_{n\in\mathcal{N}} x_{kn}(t) \leq N_k, \ \forall k \in \mathcal{K}, \tag{8d}$$

$$\sum_{n\in\mathcal{N}} x_{kn}(t) p_{kn}(t) \leq P_k^{\max}, \ \forall\, t, k \in \mathcal{K}, \tag{8e}$$

$$p_{kn}(t) \geq 0, \ \forall\, t, k \in \mathcal{K}, n \in \mathcal{N}, \tag{8f}$$

$$x_{kn}(t) \in \{0, 1\}, \ \forall\, t, k \in \mathcal{K}, n \in \mathcal{N}, \tag{8g}$$

where $\bar{p}_{kn} = \lim_{T\to\infty} \frac{1}{T}\sum_{t=1}^{T} p_{kn}(t)$ is the time-averaged power consumption of VUE pair k over RB n. (8b) is VUE k's queuing latency requirement while (8c) captures the reliability constraint of VUE k. In addition, (8d) indicates that each VUE k can be assigned up to N_k RBs. Constraint, (8e) ensures that total transmit power of VUE k over the allocated RBs is within the maximum power budget.

III. Problem Decomposition Using Lypunov Optimization

Although the optimal $\boldsymbol{X}(t)$ and $\boldsymbol{P}(t)$ can be obtained by dynamic programming, such an approach is computationally complex and requires the statistics of traffic arrivals and channel state information (CSI). To alleviate the computational complexity, we invoke tools from Lyapunov stochastic optimization [25], [27], [28] which require a partial knowledge of the CSI and provide a tractable solution compared to dynamic programming. Here, we note that, although Lyapunov

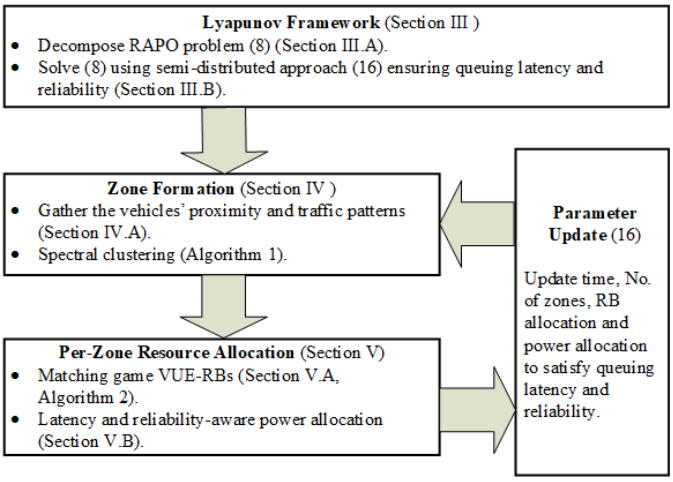

Figure 2: RAPO framework for RB allocation and power allocation.

optimization typically yields sub-optimal solutions, the optimal solution can be asymptotically approached by selecting a tradeoff parameter, as explained later in this section. The RAPO framework consists of the inter-related components as shown in Fig. 2. Using Lyapunov optimization [25], the time-average inequality constraints (8b) and (8c) can be satisfied by converting them into *virtual queues* and maintaining their stability. Therefore, we define the following virtual queue vectors $\boldsymbol{j}(t) = [j_1(t), \dots j_K(t)]$ and $\boldsymbol{f}(t) = [f_1(t), \dots f_K(t)]$ corresponding to the constraints (8b) and (8c), respectively. Accordingly, the virtual queues are updated as follows:

$$j_k(t+1) = \left[j_k(t) + q_k(t+1) - \bar{\lambda}_k d_k\right]^+, \tag{9}$$

$$f_k(t+1) = \left[f_k(t) + \mathbb{1}\{q_k(t+1) \geq L_k\} - \epsilon_k\right]^+. \tag{10}$$

We note that constraints (8b) and (8c) are satisfied if the corresponding virtual queues are *mean rate stable* [25], i.e., $\frac{1}{T}\lim_{t\to\infty}\mathbb{E}[|j_k(t)|] = 0$ and $\frac{1}{T}\lim_{t\to\infty}\mathbb{E}[|f_k(t)|] = 0, \forall\, k \in \mathcal{K}$. Hereinafter, problem in (8) is equivalent to minimizing the network-wide average transmit power subject to mean-rate stability for virtual queues.

Letting $\boldsymbol{y}(t) \triangleq [\boldsymbol{j}(t), \boldsymbol{f}(t)]$ denote a combination of the queues, we define the Lyapunov function $L(\boldsymbol{y}(t))$ and the *drift-plus-penalty* function $\Delta\big(\boldsymbol{y}(t)\big)$ as:

$$L(\boldsymbol{y}(t)) = \frac{1}{2}\Big\{\|\boldsymbol{j}(t)\|^2 + \|\boldsymbol{f}(t)\|^2\Big\}, \tag{11}$$

$$\begin{aligned}\Delta\big(\boldsymbol{y}(t)\big) &= \mathbb{E}\Big\{L\big(\boldsymbol{y}(t+1)\big) - L\big(\boldsymbol{y}(t)\big) + \sum_{n\in\mathcal{N}} v p_{kn}(t)\Big|\boldsymbol{y}(t)\Big\}, \\ &= \mathbb{E}\Big[\sum_{k\in\mathcal{K}}\Big(\frac{j_k(t+1)^2}{2} - \frac{j_k(t)^2}{2} + \frac{f_k(t+1)^2}{2} \\ &\quad - \frac{f_k(t)^2}{2} + \sum_{n\in\mathcal{N}} v p_{kn}(t)\Big)\Big|\boldsymbol{y}(t)\Big],\end{aligned} \tag{12}$$

respectively, where the parameter $v \geq 0$ controls the tradeoffs between power minimization and queue length/latency (9), (10) reduction while ensuring the stability of the queues.

Proposition 1. The conditional Lyapunov *drift-plus-penalty* (12) in time slot t satisfies the following inequality under any control strategy and queue state:

$$\begin{aligned}\Delta\big(\boldsymbol{y}(t)\big) \leq C + \mathbb{E}\Bigg[\sum_{k\in\mathcal{K}}\Big(&- \tau q_k(t) R_k(t) - \tau\lambda_k(t) R_k(t) \\ &- \tau j_k(t) R_k(t) + f_k(t)\mathbb{1}\{\big[q_k(t) + \lambda_k(t) - \tau R_k(t)\big]^+ \\ &\geq L_k\} + \sum_{n\in\mathcal{N}} v p_{kn}(t)\Big)\Big|\boldsymbol{y}(t)\Bigg]\end{aligned} \tag{13}$$

with the constant $C = \sum_{k\in\mathcal{K}}\Big(\frac{1}{2}q_k(t)^2 + \frac{1}{2}\lambda_k(t)^2 + \frac{1}{2}\tau^2 R_{k,\max}^2 + q_k(t)\lambda_k(t) + \frac{1}{2}\bar{\lambda}_k^2 d_k^2 + \frac{1}{2} + \frac{1}{2}\epsilon_k^2 + j_k(t)\max\big\{q_k(t) + \lambda_k(t), \tau R_{k,\max}\big\}\Big)$.

Proof. See Appendix A. □

Note that the solution to (8) can be found by minimizing the upper bound in (35) in each slot t [25], which is given by:

$$\begin{aligned}&\underset{\boldsymbol{X}(t),\boldsymbol{P}(t)}{\text{minimize}} \quad \sum_{k\in\mathcal{K}}\sum_{n\in\mathcal{N}} \Gamma_{kn}(t), \\ &\text{subject to} \quad \text{(8d)–(8g)},\end{aligned} \tag{14}$$

with the objective function defined as:

$$\Gamma_{kn}(t) \triangleq v p_{kn}(t) - \tau\Big(j_k(t) + f_k(t) + 2q_k(t) + 2\lambda_k(t)\Big) R_{kn}(t). \tag{15}$$

The parameter v is a non-negative constant that captures a trade-off between the optimal solution and network-wide queue stability. The optimal solution of (15) can be found as v asymptomatically increases [29].

Remark 1. *From* (14)*, we can observe that RB allocation is coupled with the power allocation problem. The formulation is an NP-hard mixed-integer programming problem which is challenging to solve [30]. Moreover, to centrally find the optimal $\boldsymbol{X}(t)$ and $\boldsymbol{P}(t)$ in each time slot, the RSU requires full global information, i.e., CSI and QSI, of the network. This is impractical for vehicular communication as the frequent exchange of local information (considering high refresh rates) between RSU and VUE pairs incurs high overhead.*

A. Semi-distributed Resource Allocation

For efficient resource allocation, the RSU needs to coordinate with the rest of the vehicles in the network in each time slot which can incur a potentially large information exchange. Furthermore, RBs are shared among VUE pairs, hence co-channel transmission from neighboring vehicles leads to severe interference. To mitigate the interference from nearby vehicles, the RSU can group the VUE pairs into a set of virtual zones[1] based on their geographic locations and traffic patterns. Therefore, instead of sending frequent vehicle's local information to RSU, we use the notion of *time scale separation* between zone formation and resource allocation, hereinafter. The RSU performs zone formation over a longer timescale,

[1]The term cluster and zone are utilized interchangeable. Furthermore, the Tx-Rx of a VUE pair is treated as a unity and grouped in the same zone during zone formation process.

and the VUE utilizes its local CSI and QSI to optimize the resource allocation and transmit power at each time slot. Thus, zone formation is a slower process than resource allocation. To this end, we assemble $T_0 \gg 1$ successive slots into one *time frame*, which is indexed by i. Thus, vehicles send their local information such as location, traffic pattern to the RSU at the beginning of each time frame instead of each time slot t. Furthermore, we assume that the RSU performs zone formation over time period T_0.

Consequently, we let $\mathcal{Z}$ be the set of Z zones. Each zone $z \in \mathcal{Z}$ is of dynamic size and changes across different time frames according to the geographical proximity and traffic patterns of VUEs. At time frame i, we denote the set of VUEs belonging to zone z as $\mathcal{K}_z(i)$. Note that $\mathcal{K}_z(i), \forall\, z \in \mathcal{Z}$, are static during one time frame but dynamic over frames. In each zone z, each VUE $k \in \mathcal{K}_z$ efficiently uses the allocated RBs while optimizing its power and satisfying (5) and (6). Furthermore, one RB cannot be shared by two VUE pairs at the same time within the same zone. We note that the restriction is imposed to avoid high interference created by the neighboring VUEs, in which case assuming that an RB can be share by multiple VUEs in the same proximity (i.e., within the zone) might be impractical as the number of VUEs scheduled at given time instance may increases. Following the idea of zone formation and resource allocation, the network-wide objective can be is written as:

$$\underset{\mathcal{Z}(i),\boldsymbol{X}(t),\boldsymbol{P}(t)}{\text{minimize}} \sum_{z\in\mathcal{Z}}\sum_{n\in\mathcal{N}_z} \Gamma_{zn}(t) \tag{16a}$$

$$\text{subject to} \sum_{k\in\mathcal{K}_z} x_{kn}(t) \le 1,\ \forall\, z \in \mathcal{Z}, n \in \mathcal{N}, \tag{16b}$$

$$\sum_{n\in\mathcal{N}} x_{kn}(t) \le N_k,\ \forall k \in \mathcal{K}_z, z \in \mathcal{Z}, \tag{16c}$$

$$x_{kn}(t) \in \{0,1\},\ \forall\, n \in \mathcal{N}, k \in \mathcal{K}_z, z \in \mathcal{Z}, \tag{16d}$$

$$\sum_{n\in\mathcal{N}} p_{kn}(t) \le P_k^{\max},\ \forall\, k \in \mathcal{K}_z, z \in \mathcal{Z}, \tag{16e}$$

$$p_{kn}(t) \ge 0,\ \forall\, n \in \mathcal{N}, k \in \mathcal{K}_z, z \in \mathcal{Z}, \tag{16f}$$

$$|\mathcal{K}_z(i)| \ge 1,\ \forall\, z \in \mathcal{Z}, \tag{16g}$$

$$\mathcal{K}_z(i) \cap \mathcal{K}_{z'}(i) = \emptyset,\ \forall\, z, z' \in \mathcal{Z},\ z \ne z', \tag{16h}$$

$$\bigcup_{z\in\mathcal{Z}} \mathcal{K}_z(i) = \mathcal{K}. \tag{16i}$$

Here, $\Gamma_{zn}(t) = \sum_{\forall k\in\mathcal{K}_z} \Gamma_{kn}(t)$ is the aggregated objective function of the VUEs in zone z. Furthermore, constraint (16b) captures the fact that a given RB n can be assigned to only one VUE $k \in \mathcal{K}_z$ inside a zone while, a VUE k can be associated to one or more RBs. Constraint (16c) states that each VUE k can be assigned up to N_k RBs. Constraints (16e)–(16h) imply that each VUE pair belongs to one zone whereas each zone has at least one VUE pair. The time-line and procedures of the proposed semi-distributed resource allocation framework are summarized in Fig. 3. Next, we present the details of traffic and proximity-aware virtual zone formation mechanism.

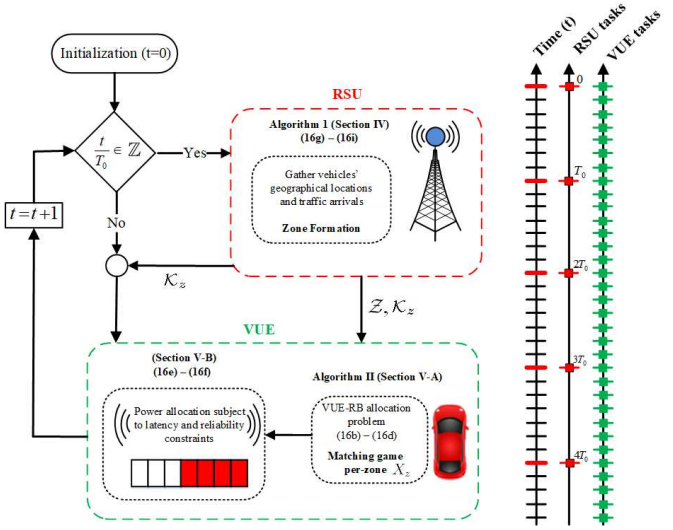

Figure 3: Timeline and procedures of the zone formation and resource allocation framework.

IV. Proposed Solution Using Zone Formation

The problem in (16) is centralized and combinatorial in nature with exponential complexity. Developing a semi-distributed approach in which limited control data exchange is needed between VUEs and RSU is desirable. Furthermore, the proposed approach requires minimal coordination[2] between neighboring VUEs. Hence, to mitigate interference and minimize overhead caused by signaling, we cluster VUEs based on similar attributes. This will allow to perform coordination between VUEs with little signaling overhead. There are numerous similarity features that impact interference between VUEs. Two key factors are their physical distance and traffic arrival patterns. In this regard, we use geographical information and traffic arrival similarities to group VUEs into distinct zones. Therefore, we introduced a dynamic zone-formation strategy, which takes into account both the physical proximity of VUEs and their traffic patterns (e.g., traffic arrival, interference). Moreover, the zone size varies dynamically (with respect to time) depending on the dynamic nature of VUE traffic arrival and their proximity. The set of zones is partitioned into $|Z|$ non-overlapping zones, such that:

$$\bigcup_{\forall z\in\mathcal{Z}} \mathcal{K}_z = \mathcal{K} \text{ and } \mathcal{K}_z \cap \mathcal{K}_{z'} = \emptyset,\ \forall\, z \ne z'. \tag{17}$$

Let us assume $G = (\mathcal{K}, \mathcal{E})$ denote as an undirected graph, where $\mathcal{K}$ is the set of VUE pairs (vertices of graph) and $\mathcal{E} \subset \mathcal{K} \times \mathcal{K}$ be the set of links between locally-coupled VUEs pairs in terms of their physical distance and traffic arrivals.

A. Similarity based VUE Zone formation

Given the graph $G = (\mathcal{K}, \mathcal{E})$, let $\boldsymbol{s}_k$ and $\boldsymbol{s}_{k'}$ be the geographical coordinates of the V-UE pairs k and k' respectively, in Euclidean space. Here, we define parameter ϵ_s to represent

[2]We note that by incorporating the transmission radius, we can minimize the coordination area.

the presence of a link or edge $e \in \mathcal{E}$ between neighboring VUEs k and k' such that $\{e_{s_{kk'}} = e_{s_{k'k}} = 1, ||\boldsymbol{s}_k - \boldsymbol{s}_{k'}|| \leq \delta\}$. In other words δ represents the coordination radius for VUE. The geographical locations of vehicles do not change significantly during one time frame. Therefore, average locations of vehicles are considered. The Gaussian distance similarity is based on the distance between two VUEs k and k' which is given as [31]:

$$s_{kk'}(i) = \begin{cases} \exp\left(\frac{-||\boldsymbol{s}_k - \boldsymbol{s}_{k'}||^2}{2\sigma_s^2}\right), & \text{if } \|\boldsymbol{s}_k - \boldsymbol{s}_{k'}\| \leq \delta, \\ 0, & \text{otherwise.} \end{cases} \tag{18}$$

Here, the parameter σ_s controls the impact of the neighborhood size. For a given δ, the range of the Gaussian distance dissimilarity for any two close-by VUE pairs is $[1, e^{-\delta/2\sigma_s^2}]$, where the lower bound is determined by σ_s. Furthermore, $\boldsymbol{S}$ represents the distance-based similarity matrix with each entry $s_{kk'}(i)$ given by (18).

Comparing the variation in geographical location of VUEs pairs in (18), the traffic patterns of VUEs vary frequently over time. Since, time-varying location and traffic arrivals of vehicles are two important *dynamic* aspects therefore, grouping VUEs pairs based on their temporal location and traffic aspects makes the zone formation dynamic. As described in Section III-A for the zone formation performed over the longer time period, we exploit the correlation of the traffic among subsequent time slots, and thus the estimated time average traffic arrival $\hat{\lambda}_k$ for each VUE k is observed.

$$\hat{\lambda}_k = \sum_{t=1}^{(i-1)T_0} \frac{\lambda_k(t)}{(i-1)T_0}, \tag{19}$$

Let $c_{kk'}(i)$ be an entry of the Gaussian traffic arrival dissimilarity matrix $\boldsymbol{C}$ between VUEs $k, k' \in \mathcal{K}$ with respect to their traffic arrivals $\hat{\lambda}_k$ and $\hat{\lambda}_{k'}$, which is given [31]:

$$c_{kk'}(i) = \exp\left(\frac{||\hat{\lambda}_k - \hat{\lambda}_{k'}||^2}{2\sigma_l^2}\right), \tag{20}$$

Here σ_l parameter controls the impact of traffic arrival on the dissimilarity. The upper bound of the dissimilarity is based on the choice of σ_l.

The key step in zone formation is to identify similarities between VUEs pairs to group VUEs with similar characteristics. In order to reuse resources between virtual zones grouping VUEs pairs having different traffic patterns and physically nearby, we combine the traffic arrival and distance similarities. A Gaussian affinity matrix $\boldsymbol{A}$ that blends time-average traffic affinity with spatial proximity is:

$$\boldsymbol{A} = (\boldsymbol{S})^{\theta}.(\boldsymbol{C})^{(1-\theta)}, \tag{21}$$

where $0 \leq \theta \leq 1$ controls the impact of traffic arrival and distance similarity. A spectral clustering algorithm (Algorithm 1) is used to construct zones between VUEs based on their Gaussian affinity matrix $\boldsymbol{A}$. Grouping dissimilar VUEs in terms of geographical distance and traffic patterns similarities as (18) and (20), respectively, mitigates interference and thus, minimizes the total network cost.

Algorithm 1 Spectral clustering for zone formation [31]

1: **Initialization**: Read the time frame index i of length T_0, calculate affinity matrix $\boldsymbol{A} = [a_{jx}]$ as in (21) of a graph $\mathcal{G}$, choose $b_{\text{min}} = 2$ and $b_{\text{max}} = K/2$.
2: Compute diagonal degree matrix $\boldsymbol{M}$ with diagonal $m_j = \sum_{x=1}^{K} a_{jx}$.
3: $\boldsymbol{L} = \boldsymbol{M} - \boldsymbol{A}$.
4: $\boldsymbol{L}_{\text{norm}} := \boldsymbol{M}^{-1/2}\boldsymbol{L}\boldsymbol{M}^{-1/2}$.
5: Pick a number of b_{max} eigenvalues of $\boldsymbol{L}_{norm}$ such that $\rho_1 \leq, \ldots, \leq \rho_{k_{\text{max}}}$.
6: Choose $B = \max_{j=b_{\text{min}},\ldots,b_{\text{max}}} \Delta_j$ where $\Delta_i = \rho_{j+1} - \rho_j$.
7: Choose the b smallest eigenvectors $w_1, ..., w_b$ of $\boldsymbol{L}_{\text{norm}}$.
8: Let $\boldsymbol{W}$ matrix has the eigenvectors $w_1, \ldots w_b$ as columns.
9: Use k-means clustering to cluster (zone) the rows of matrix $\boldsymbol{W}$.
10: Zone set $\{1, ..., Z_{|\mathcal{Z}|}\}$.

B. Coordination

Zone formation reduces the signaling overhead required for coordination among VUEs and RSU as compared to a centralized approach. However, the interference $I_{kn}(t)$ in $\Gamma_{zn}(t)$ of problem (16) (as per (1), (3), and (15)) contains intra and inter-zone interference, i.e., $I_{kn}(t) = I_{kn}^{\text{intra-zone}}(t) + I_{kn}^{\text{inter-zone}}(t)$ and defined as:

$$I_{kn}^{\text{intra-zone}}(t) = \sum_{k' \in \mathcal{K}_z \setminus k} x_{k'n}(t) p_{k'n}(t) |h_{k'kn}(t)|^2, \tag{22}$$

$$I_{kn}^{\text{inter-zone}}(t) = \sum_{k'' \in \mathcal{K} \setminus \mathcal{K}_z} x_{k''n}(t) p_{k''n}(t) |h_{k''kn}(t)|^2. \tag{23}$$

Prior to solving the proposed RAPO problem, in (16b)–(16i), we note that the solution of the network problem depends on the resource allocation and power optimization solution due to the fact that optimizing the power of each VUE pair depends on the allocated RBs. Moreover, to allocate the resources to each VUE pair, interference must be considered. Since RB allocation is coupled with power allocation, we propose a novel approach that solve the RAPO problem.

However, solving (16) requires the knowledge of all zones i.e., $\boldsymbol{X}(t), \boldsymbol{P}(t)$, and interference (22), (23) in the network, which can be complex and not practical. Therefore, we decouple the RB allocation from the power allocation problem. First, a low complexity matching algorithm is proposed that matches RBs to the VUEs inside each zone. Given the outcome of the matching, a power allocation problem is proposed to optimally allocate power to VUEs over the matched RBs.

V. Per-Zone RB Allocation And Power Allocation

Our objective is to develop a self-organizing mechanism to solve the RAPO problem in (16) using a semi-decentralized approach in which VUEs inside each zone interact and make resource allocation decision. First, the resource allocation problem is formulated as a matching game per-zone between VUEs and RBs by allocating equal power. To solve the resource allocation problem at RSU, while taking into account dynamic channel characteristics an inter-zone interference

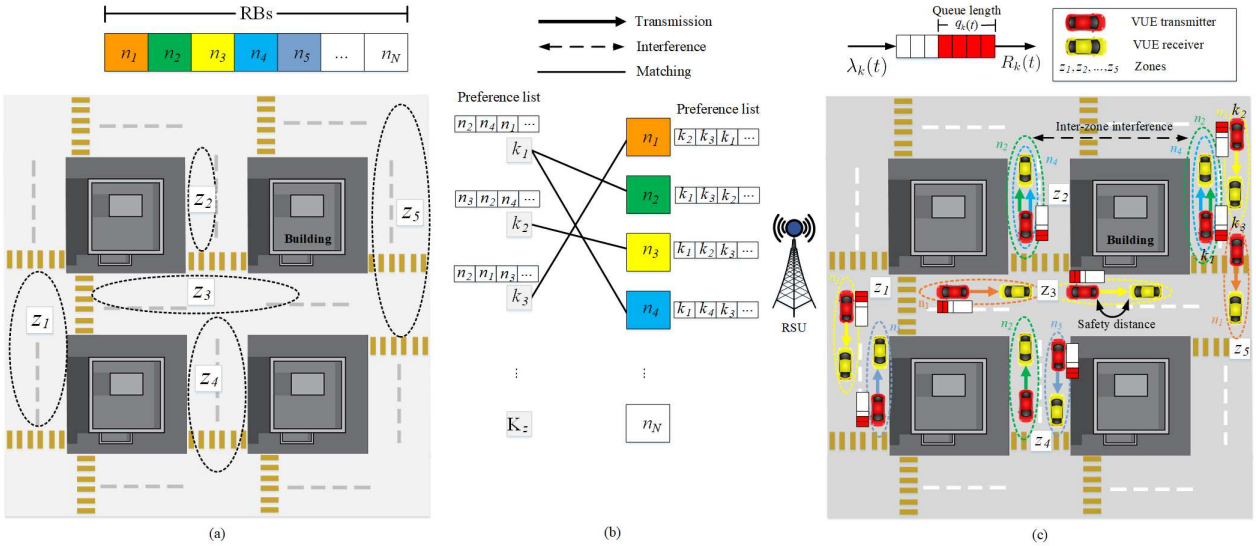

Figure 4: (a) RSU-assisted zone formation among VUE pairs, (b) Per-zone VUE-RB matching in which VUE and RB preferences are based on their utility, (c) Inter-zone interference and power allocation for V2V transmissions.

estimation method is proposed. Subsequently a matching algorithm is proposed in order to find the suitable VUE-RBs allocation. Then, power allocation is performed at each VUE over the allocated RBs.

A. VUE-RB Matching

1) Matching preliminaries: To overcome the combinatorial nature of the RB allocation problem (16b)–(16d), we utilize the framework of matching theory [32]–[35]. A matching game per-zone $X_z : \mathcal{K}_z \rightarrow \mathcal{N}$ is essentially a two-sided assignment problem between two disjoint sets of players, e.g., the set of VUEs $\mathcal{K}_z$ and the set of RBs $\mathcal{N}$, in which the players of one set tries to match (associate) to the most suitable players of the other set according to their own *preference relations*. Further, for a *one-to-many* matching game, each player in $\mathcal{K}_z$ is matched to one or multiple players in $\mathcal{N}$ whereas each player in $\mathcal{N}$ is matched to at most one player in $\mathcal{K}_z$. The preferences of the sets of VUEs and RBs $(\mathcal{K}_z, \mathcal{N})$ denoted by $\succ_k$ and $\succ_n$, respectively, represents ranking of players from one set over the other set.

Definition 1. Given two disjoint sets of finite players $\mathcal{K}_z$ and $\mathcal{N}$, a *one-to-many* matching X_z is defined as a mapping from the set $\mathcal{K}_z \cup \mathcal{N}$ into the set of all subsets of $\mathcal{N} \cup \mathcal{K}_z$ such that for each $k \in \mathcal{K}_z$ and $n \in \mathcal{N}$: 1) $X_z(k) \subseteq \mathcal{N}$; 2) $X_z(n) \in \mathcal{K}_z$; 3) $X_z(k) \leq N_k$; 4)$X_z(n) \leq 1$; 5) $X_z(n) = \{k\} \Leftrightarrow n \in X_z(k)$. Note from 3) that a VUE is matched to at most a quota of N_k RBs, whereas from 4) that RBs are matched to at most one VUE within give zone $\forall k \in \mathcal{K}_z$.

In the proposed matching, the quota of the VUE is changing with time but will be fixed over a given time slot. The notion of quota N_k for the VUE k accounts the queue length, latency and reliability constraints as per (4), (5) and (6), respectively. That is, a VUE pair with a tighter constraints (lower L_k and ϵ_k) or VUE k with higher traffic demand $\bar{\lambda}_k$ will need more RBs to flash the data from its queue buffer. Hence, by utilizing L_k, ϵ_k, and $\bar{\lambda}_k$, $\forall\, k \in \mathcal{K}_z$, the quota of a VUE pair k is determined using the following proportional fairness metric:

$$N_k = \frac{N \times \frac{q_k(t)\bar{\lambda}_k}{L_k \epsilon_k}}{\sum_{k \in \mathcal{K}_z} \frac{q_k(t)\bar{\lambda}_k}{L_k \epsilon_k}}. \tag{24}$$

The main goal of a matching problem is to optimally match two sets of players (i.e., $\mathcal{K}_z$ and $\mathcal{N}$), given their individual utilities which are captured by objective functions as per (25) and (26). More interestingly, the matching framework allows defining the relevant utility per VUE and RB, which captures the preferences of VUEs and RBs. In this regard, the utility that an arbitrary VUE $k \in \mathcal{K}_z$ is assigned an RB $n \in \mathcal{N}$ is given by:

$$U_k(t) = -\sum_{n \in \mathcal{N}} \Gamma_{kn}(t). \tag{25}$$

Accordingly, the utility of an RB assigned to a VUE k is:

$$U_{kn}(t) = -\Gamma_{kn}(t). \tag{26}$$

Hereinafter, we ignore the time index t in utilities for notational simplicity.

Definition 2. A *preference relation* $\succ$ is defined as a complete, reflexive and transitive binary relation between players in $\mathcal{K}_z$ and $\mathcal{N}$. In particular, if $n \succ_k n'$ and $n' \succ_k n''$, then $n \succ_k n''$ similarly, if $k \succ_n k'$ and $k' \succ_n k''$, then $k \succ_n k''$.

Each VUE aims to maximize its own utility while maintaining its queues stability through optimizing its RB selection. Therefore, each VUE $k \in \mathcal{K}_z$ ranks the subset of the proposing RBs i.e., $\mathcal{P} \subseteq \mathcal{N}$ and $\mathcal{P}' \subseteq \mathcal{N}$. Essentially, we can define the preference profile of a VUE k, $\succ_k$ as follows:

$$\mathcal{P} \succ_k \mathcal{P}' \Longleftrightarrow U_k(\mathcal{P}) > U_k(\mathcal{P}'). \tag{27}$$

On the other hand, each RB n rank the VUEs $k, k' \in \mathcal{K}_z, k \neq k'$ based on the preference $\succ_n$ to maximize its own utility,

which is expressed as:

$$k \succ_n k' \Longleftrightarrow U_{kn} > U_{k'n}. \tag{28}$$

The preference of players in the given matching depends on intra-zone and inter-zone interference as per (22) and (23), respectively. Note that, the proposed VUE-RB matching game satisfies constraints (16b)–(16d). Therefore, in order to perform a proper resource allocation, VUE needs to communicate within the zone and outside zone. Considering the vehicular network with very large control information among vehicles, rendering matching algorithm is impractical.

Having defined the proposed VUE-RB matching, (16b) constraint eliminates the intra-zone interference. To address the inter-zone interference, each VUE estimates interference based on its time-weighted history. While considering temporal and location-aware nature of vehicular networks, the latest information on interfering vehicles is given more weight during resource allocation. Therefore, we consider an unbiased estimator[3] for $\hat{I}_{kn}^{\text{inter-zone}}(t)$:

$$\hat{I}_{kn}^{\text{inter-zone}}(t) = \frac{1+\alpha}{1+\alpha^{i-1}} \sum_{\kappa=1}^{i-1} \alpha^{i-1-\kappa} \sum_{t=(\kappa-1)T_0+1}^{\kappa T_0} \frac{I_{kn}^{\text{inter-zone}}(t)}{T_0}. \tag{29}$$

Hence, a parameter $0 \leq \alpha < 1$ is used in order to give weight to the inter-zone interference in the temporal domain and defined as the sum of a geometric sequence with a scale factor $(1+\alpha)/(1+\alpha^{i-1})$.

Once the estimated utilities are calculated, the preference profile of players is derived from the estimated terms. The preference of VUE k over two subsets of RBs $\mathcal{P} \subseteq \mathcal{N}$ and $\mathcal{P}' \subseteq \mathcal{N}$ is:

$$\mathcal{P} \succ_k \mathcal{P}' \Leftrightarrow \hat{U}_k(\mathcal{P}) > \hat{U}_k(\mathcal{P}'). \tag{30}$$

Subsequently, preference profiles are build for RBs over the VUEs using the estimated inter-zone interference denoted as $\hat{U}_{kn}$. Hence, an VUE's preference over RBs within a zone z is given by:

$$k \succ_n k' \Leftrightarrow \hat{U}_{kn} > \hat{U}_{k'n}. \tag{31}$$

Using this formulation, we develop an algorithmic solution for the proposed matching game that allows finding the suitable VUE-RB matching.

2) Proposed VUE-RB Allocation Algorithm: To solve the formulated game and find the suitable network VUE-RB matching X_z, we consider two important concepts: *two-sided stability* and *Pareto optimality*. A two sided stable is essentially a solution concept that can be used to characterize the outcome of a matching game. In particular, two-sided stability is defined as follows [32]:

Definition 3. A pair (k,n) such that $k \in \mathcal{K}_z$ and $n \in \mathcal{N}$, in zone matching $X_z, (k,n) \in X_z$ is a *blocking pair* if and only if $n \succ_k X_z(k)$ and $k \succ_n k'$ for some $k' \in X_z(n)$. A matching X_z said to be *two-sided stable*, if there is no blocking pair,.

[3]It is noted that for given instance of matching the estimated inter-zone interference is considered constant, which does not affects the player's preference.

Algorithm 2 Per-zone VUE-RB Matching Algorithm

Initialization: Set all RBs unmatched and initialize VUEs with empty lists of proposals.
Construct preference lists for RBs using (27).
repeat each unmatched RB
    proposed to its most preferred VUE.
  for each VUE j **do**
    Observe the subset of RBs that are in j's proposal list: $\mathcal{P}_j$.
    if $|\mathcal{P}_j| = 1$, **then**
      Accept RB in $\mathcal{P}_j$.
    else if $|\mathcal{P}_j| = 2$, **then**
      if $\mathcal{P}_j \succ_k \mathcal{P}'_j,\ \forall \mathcal{P}'_j \subseteq \mathcal{P}_j$ **then**
        Accept both RBs.
      else
        Accept the most preferred RB in $\mathcal{P}'_j$ and reject the other.
      end if
    else if $|\mathcal{P}_j| > 2$, **then**
      Identify feasible subset (FS) of j as $\mathcal{P}'_j \subseteq \mathcal{P}_j$ that satisfies constraints (16b)–(16d).
      Calculate j's preference over all FS.
      Accept RBs in the most preferred subset of j and reject other RBs.
    end if
    Mark an accepted RB as matched.
    Remove j from rejected RB's preference list.
  end for
until either all RBs are matched or no VUE remains in their preference lists.
Output: a stable pair-wise matching X_z.

The notion of two-sided stability ensures fairness for the VUE-RB allocation. That is, if a VUE k prefers the assignment of another VUE k', then k' must be preferred by the $X_z(k')$ to k, otherwise, X_z will not be two-sided stable. Two-sided stability characterizes the stability and fairness of the matching problem, while Pareto optimality characterized the efficiency of the solution, as defined next:

Definition 4. A matching game X_z isa said to be *Pareto optimal (PO)*, if there is no other matching X'_z such that X'_z is equally preferred to X_z by all the VUEs, $X'_z(k) \succeq_k X_z(k), \forall k \in \mathcal{K}_z$, and strictly preferred over X_z, $X'_z \succ_k X_z(k)$ for some VUEs.

In order to find the stable solution of the proposed matching game, the so-called *deferred acceptance (DA)* algorithm is adopted [36]. Subsequently, a DA-based algorithm (shown in Algorithm 2) that proceeds as follows. Following each round of the proposed algorithm, each unmatched RB proposes to its most preferred VUE in its preference list. Based on the proposal, VUEs accept or reject the offers. As a matter of fact, a VUE only accepts those RBs which leads to maximizing its own utility and reject others and thus, it also removes blocking pairs possibility. Different steps of matching algorithm and its flow is presented in Algorithm 2. Since it is based on a variant

of the DA process, Algorithm 2 is guaranteed to converge to a stable matching as shown in [36]. Moreover, among the set of all stable solutions, Algorithm 2 yields the solution that is PO for the RBs. Here we note that the VUE will change location and QSI dynamically over time. However, a given zone is static within a time frame while RB allocation is executed at each time slot depending on CSI and estimated inter-zone interference. The proposed solution in Algorithm 2 allows the VUEs to update their preference profiles, that depend on their achieved utilities for each matched set of RBs and vice-versa. Given X_z resulting from Algorithm 2, each VUE $k \in \mathcal{K}_z$ must be assigned to the RBs in $X_z(k)$. Next, we discuss some key properties for Algorithm 2.

Remark 2. *Algorithm 2 is guaranteed to converge to a two-sided stable matching X_z between VUEs and RBs. Moreover, the resulting solution, among all possible stable matchings, is Pareto optimal for VUEs.*

Algorithm 2 will always converge, since no RBs will apply for the same VUE more than once. Furthermore, we note that the proposed solution is Pareto optimal within each zone, corresponding to each step in Algorithm 2, an it is assumed that zones formation will not effect the utility functions. This assumption is valid, since a given RB will experience random interference from the interfering VUEs. Given that the zone formation happened after each T_0, the average interference power will be fixed during T_0. Hence, the preference profiles of the RBs and VUEs, and consequent matching within each zone will be independent of all other zones. Therefore, the matching within each zone is Pareto optimal and maximize over all players utilities as per (25) and (26). To this end, we next propose a latency and reliability-aware power allocation solution.

B. Latency and Reliability-aware Power Allocation at the VUE

After the subset of RBs $\mathcal{N}_k$ is allocated to the VUEs inside zone z, each VUE $k \in \mathcal{K}_z$ inside its respective zone z optimizes the transmit power over the allocated RBs, i.e., $\mathcal{N}_k$. The optimal power allocation is performed locally by each VUE pair. Thus, given the RBs allocated by the matching algorithm, the local power allocation can be written as a convex optimization problem:

$$\underset{p_{kn}}{\text{minimize}} \quad \sum_{n\in\mathcal{N}_k} v p_{kn} - \sum_{n\in\mathcal{N}_k} \tau\omega\big(j_k + f_k + 2q_k + 2\lambda_k\big) \times \mathbb{E}_{I_{kn}^{\text{inter-zone}}}\left[\log_2\left(1 + \frac{p_{kn}|h_{kkn}|^2}{\sigma^2 + I_{kn}^{\text{inter-zone}}}\right)\right] \tag{32a}$$

$$\text{subject to} \quad \sum_{n\in\mathcal{N}_k} p_{kn} \le P_k^{\max}, \ \forall k \in \mathcal{K}_z \tag{32b}$$

$$p_{kn} \ge 0, \ \forall n \in \mathcal{N}_k, \tag{32c}$$

which is solved in each time instant although we omit the time index t for notational simplicity. Here, $\mathbb{E}[\cdot]$ is the expectation with respect to the inter-zone interference (23). We note that CSI and QSI are utilized locally to solve (32) for power allocation. This substantially reduces the overheads of reporting local information to the RSU, as compared to the fully-centralized approach. The optimal solution to problem (32) is detailed in the following Lemma.

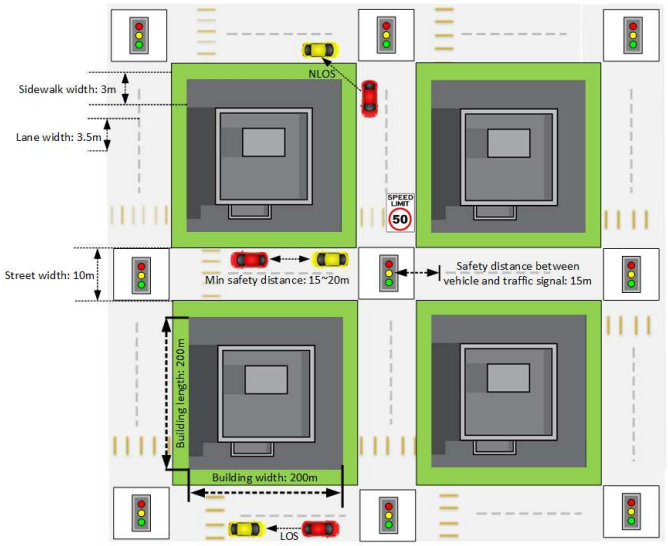

Figure 5: Road configuration for Manhattan model

Lemma 1. For all $n \in \mathcal{N}_k$, if $\frac{\tau\omega\left(j_k+f_k+2q_k+2\lambda_k\right)}{\ln 2} \times \mathbb{E}\left[\frac{h_{kkn}}{\sigma^2+I_{kn}^{\text{inter-zone}}}\right] > v + \gamma$, we find the optimal transmit power $p_{kn}^* > 0$ such that

$$\frac{\tau\big(j_k + f_k + 2q_k + 2\lambda_k\big)}{\ln 2} \times \mathbb{E}\left[\frac{h_{kkn}}{\sigma^2 + I_{kn}^{\text{inter-zone}} + p_{kn}^* h_{kkn}}\right] = v + \gamma. \tag{33}$$

Otherwise, $p_{kn}^* = 0$. Moreover, the Lagrange multiplier γ is 0 if $\sum_{n\in\mathcal{N}_k} p_{kn}^* < P_k^{\max}$, and we have $\sum_{n\in\mathcal{N}_k} p_{kn}^* = P_k^{\max}$ when $\gamma > 0$.

Proof. Please refer to Appendix B. □

In (33), we can see that when j_k, f_k, q_k, or λ_k is large, the reliability constraint (7) can be easily violated due to a large queue length and data arrival (as per (4) and (10)). Therefore, in order to satisfy (5) and (6), each VUE minimizes the transmit power. Otherwise, power consumption is minimized. After sending information, each VUE pair k updates $q_k(t+1)$, $j_k(t+1)$ and $f_k(t+1)$ as per (4), (9) and (10) respectively.

VI. Simulation Results and Analysis

In order to evaluate the performance of our proposed scheme, we have simulated a Manhattan mobility model with various densities of vehicles. The VUE pairs are distributed over the specified traffic lanes covering area of $460 \times 460\,\text{m}^2$. Fig. 5 shows the simulation area setup considering four buildings and bi-directional traffic lanes. Each building considered to be a fixed breadth of 200 m. Moreover, four different kind of vehicles Audi (A3, A4, A5 and A6) with their specified length and width are considered[4].

[4]https://www.automobiledimension.com/audi-car-dimensions.html

Table III: Simulation Parameters

Parameter	**Value**
Carrier frequency	6 GHz [37]
RB bandwidth	180 kHz
V-UE Tx/Rx antenna height	1.5 m
Building breadth	200 m
Distance between traffic signal and vehicle	15 m
Lane width	3.5 m
Vehicle Type (Audi)	A3, A4, A5, A6
Noise power spectral density N_0	-174 dBm/Hz
Minimum safety distance	[15 m - 20 m]
Vehicle average speed	50 km/h
V-UE transmission power	10 dBm
Fading model	Rayleigh fading
Allowable queue length L_k	3.3 kbps
Tolerable violation probability ϵ_k	0.1
Weight parameter α	0.033
Impact of traffic arrival σ_l^2	341.73
Impact of neighborhood size (distance) σ_s^2	49.71
Neighborhood radius δ	90 m
Impact of distance and traffic arrival on similarity θ	0.5
$b_{\min}$, $b_{\max}$ parameters for zone formation	2, $\lceil (K/2)+1 \rceil$

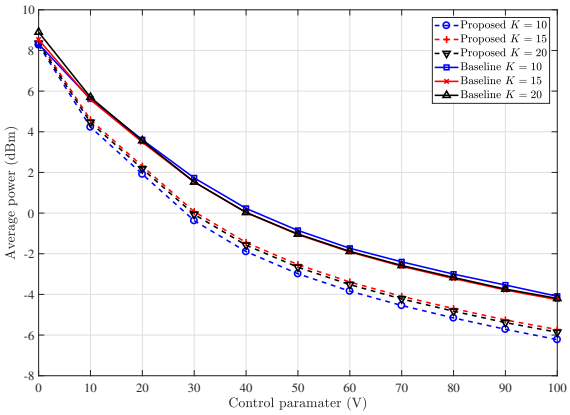

Figure 6: Tradeoff between average power and control parameter V for various densities of VUEs with fixed RBs $N = 15$.

Vehicles moves along pre-defined bi-directional lanes with the average speed of 50 km/h. Minimum safety distance between the VUE' transmitter and VUE' receiver dynamically ranges from 15 m to 20 m. In order to make our simulations closer to realistic mobility and avoid collisions among vehicles, traffic signals are emulated at each intersection area. Whenever a vehicle reaches the traffic signal, it randomly chooses a direction based on the possible options (north/west/east/south). Event-trigged traffic messages modeled by Poisson process with mean arrival rate of $\mu = 75$ bytes are transmitted at every time slot [38]. The V2V line of sight (LOS) and non-line of sight (NLOS) WINNER+B1 channel model for the Manhattan layout is considered for path loss calculation [37]. For every VUE pair $k \in \mathcal{K}$, we set RBs $N = 15$, $P_k^{\max} = 10\,\text{dBm}$, $\bar{\lambda}_k = 200\,\text{kbps}$, $L_k = 3.3\,\text{kbps}$, and $\epsilon_k = 0.1$. The other parameters are: $N = 15$ RBs, $\omega = 180\,\text{kHz}$, $\tau = 3\,\text{ms}$, $T_0 = 10$. The simulation parameters are given in Table III. To compare the proposed approach with 3GPP baseline [39] (*configuration 1, distributed scheduling*), each VUE pair optimizes its power over all RBs in every time slot. We use $Q_k(t)/\lambda_k(t)$ as the instantaneous queuing latency metric [40], $\bar{Q}/\bar{\lambda}$ as the average queuing latency [26].

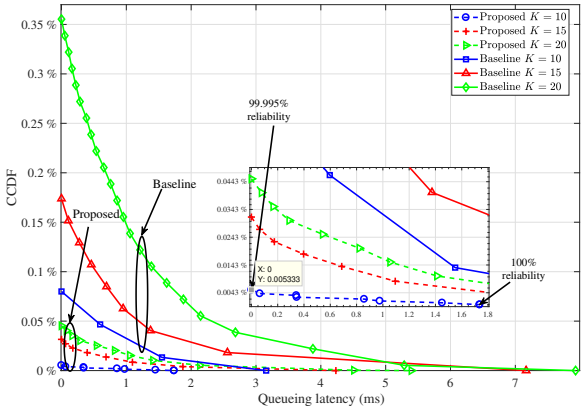

Figure 7: CCDF of the instantaneous queuing latency for different densities of VUEs with fixed $V = 0$ and $N = 15$.

Table IV: Latency reduction and reliability improvement

QoS \ VUEs	$K = 10$	$K = 15$	$K = 20$
Latency reduction ↓	45%	41%	32%
Reliability improvement ↑	94%	82%	87%

A. *Impact of VUE density*

The tradeoff between the average power consumption and control parameter V is shown in Fig. 6 for different densities of VUE pairs. When V is smaller as per (32a), the VUE focuses on the rate maximization which consumes more power. In contrast, for a larger V, the VUE reduce its power consumption by allowing the queue length to grow. Fig. 6 also shows that the proposed approach yields significant reduction in power for higher values of V over the baseline approach. Fig. 6 shows that, at $V = 0$ proposed approach yields 0.5%, 1% and 6.6% reduction in average power for VUE densities of 10, 15 and 20, respectively. Meanwhile, at $V = 100$ the proposed approach outperforms the baseline and reduces the average power by up to 34.2%, 25.7% and 28.4% for $K = 10, 15$, and 20, respectively.

Subsequently, when V is smaller as per (32), each VUE will focus on rate maximization to decrease its queuing latency thus consuming more power. Considering the case $V = 0$, we investigate the transmission reliability via the complementary cumulative distribution function (CCDF) of the instantaneous queuing latency. The reliability performance for varying VUE densities is shown in Fig. 7. It can be seen that, for different network settings, our approach always satisfies the aforementioned latency and reliability constraint as per (5) and (6) while achieving a higher reliability performance (i.e., lower CCDF values) compared with the baseline. Table IV shows that our proposed scheme outperforms the baseline with

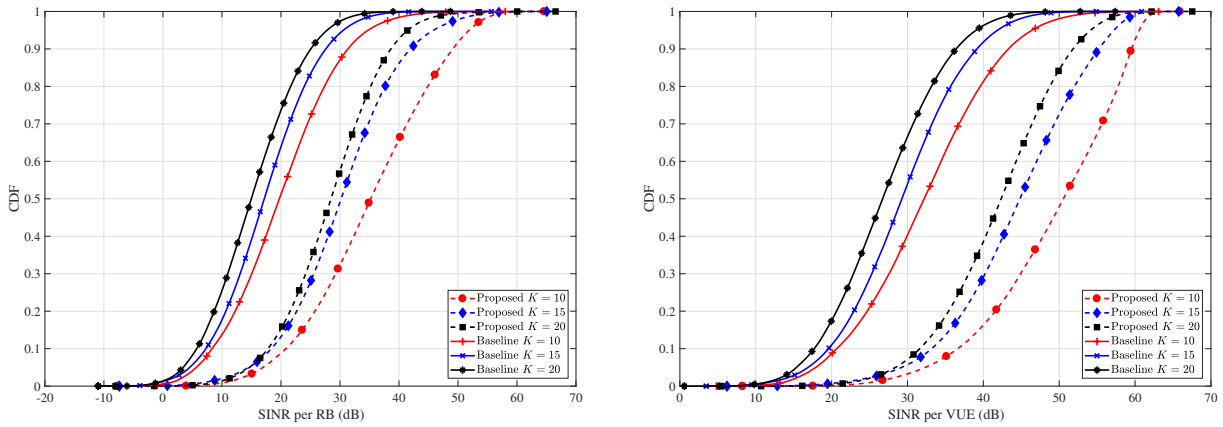

Figure 8: Cumulative density function of SINR with fixed $V = 0$, $N = 15$, and different densities of VUEs under the considered approaches.

an average queuing latency reduction and achieves significant improvement in term of reliability for different densities of VUEs. Furthermore, from the Fig. 7, at 0.0053% of the CCDF value (i.e., 99.995% reliability) our proposed approach achieves a queuing latency reduction by up to 100%, 72%, and 60% for $K = 10, 15$, and 20, respectively, as compared to the baseline.

Fig. 8 shows the cumulative density function of SINR and VUE's SINR for different densities of VUEs $K = 10$, 15 and 20, for a fixed value of $V = 0$. Fig. 8 shows a significant gain in SINR for the proposed approach compared to the baseline. That is due to the fact that zone formation and matching can help mitigates interference. In the proposed approach, a VUE can use one or multiple RBs based on its traffic demand to satisfy its QoS. The quota of a VUE defines the maximum number of RBs a VUE can use, whereas, in the baseline, the VUEs utilize all RBs and optimize their transmission power. In a scenario with relative high load (e.g., for $K = 20$), the performance gap between the baseline and the proposed RAPO is more significant. This is due to the fact that interference increases with the increase in the number of VUEs.

B. Impact of queuing latency

We show impact of the parameters ϵ_k and L_k on the queuing latency. Fig. 9 shows the effect of ϵ_k for a fixed number of VUE pairs $K = 20$ and RBs $N = 15$. In order to analyze the performance of queuing latency for different values of ϵ_k, we consider the case in which $K > N$, for a fixed value of $L_k = 2$. From Fig. 9, we can see that, in order to achieve a 99.995% reliability (i.e., 0.0053% of CCDF) for different values of ϵ_k, the proposed approach reduces queuing latency as compared to baseline by up to 80% and 77% for $\epsilon = 0.1$ and 1.0, respectively.

Fig. 10 shows the effect of L_k for a $K = 20$ VUE pairs and $N = 15$ RBs. In order to examine the performance of queuing latency for different values of L_k, we consider the case in which $K > N$ and $\epsilon = 0.1$. Fig. 10 shows that, in order to achieve 99.995% reliability for different values of L_k, the proposed approach reduces queuing latency by up to 79%

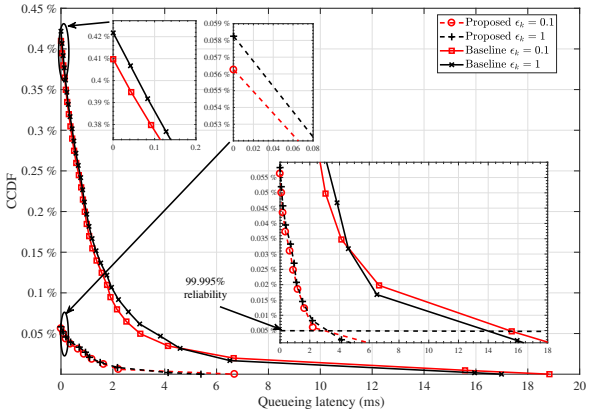

Figure 9: CCDF of the instantaneous queuing latency for different ϵ_k with fixed $V = 0$, $N = 15$, $L_k = 2$, and $K = 20$ VUE pairs.

and 74% for $L_k = 2$ and 8, respectively, as compared to the baseline.

C. Impact of Clustering

In Fig. 11, we present the impact of the neighborhood range on the average queuing latency for VUEs $K = 15$ and 20. We vary the neighborhood discovery δ range from 70 m to 130 m. From Fig. 11, we can observe that the average queuing latency decrease when the neighborhood discovery radius increases. This is due to the fact that, as we increase the zone radius spacing, interference among the zones decreases. The average queuing latency is higher when the number of VUEs pairs increases. Furthermore, by increasing the neighborhood radius from 70 m to 130 m the proposed approach reduces queuing latency by up to 47% and 203%, for VUEs $K = 15$ and 20, respectively.

In Fig. 12, we present the average number of zones and the average zone sizes of VUEs. We use $K = 20$ VUEs and $N = 15$ RBs with the neighborhood discovery range δ

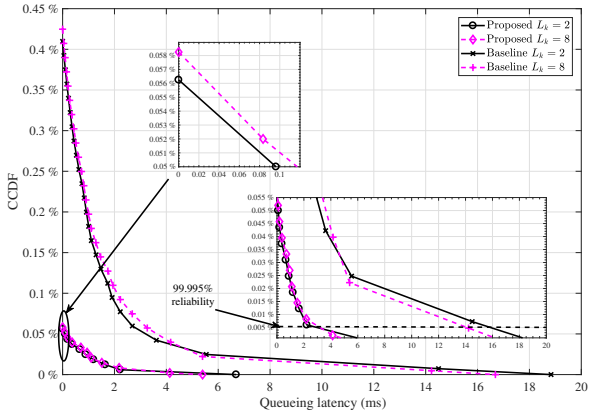

Figure 10: CCDF of the instantaneous queuing latency for different L_k with $\epsilon_k = 0.1$, $V = 0$, $N = 15$, and $K = 20$ VUE pairs.

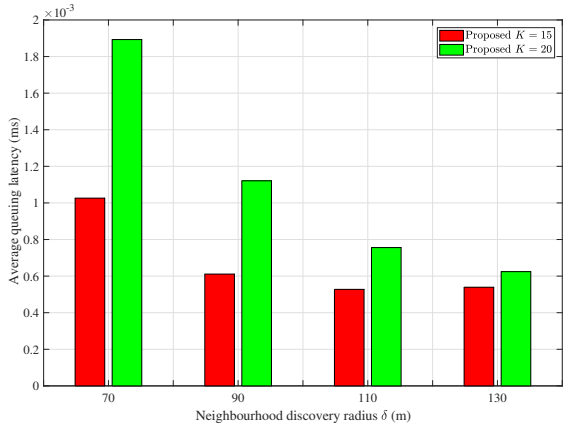

Figure 11: Neighborhood discovery radius vs. latency for a fixed number of VUEs $K = 20$, $V = 0$, and $N = 15$.

varying fom 40 m to 140 m. Fig. 12 shows the impact of distance, traffic arrival, and joint similarity on the coordination of VUEs to form zones as per in (21). For the joint similarity, θ is set to 0.5. As per (18)–(21). Fig. 12, shows that zone formation based on the distance similarity allows to group more VUEs together yielding a smaller number of zones and a larger average zone size. Since we consider the mean arrival rate, the effect of arrival rate is constant when considering only the arrival rate for the zone formation. This is due to the fact that, we consider the mean arrival rate which should be the same in average over time. The increase in zone size directly influences the zone load. Furthermore, zone formation based on the joint similarity takes into account distance as well as traffic arrival similarities to form zones.

VII. Conclusion

In this work, we have proposed a new scheme for power and RBs allocation in V2V communication while satisfying queuing latency and reliability constraints. To solve the proposed problem, we have introduced a novel two-timescale

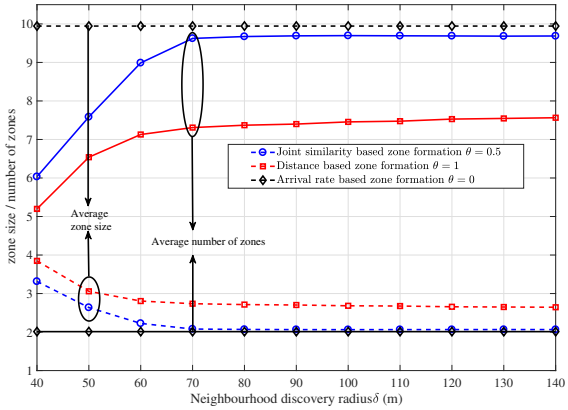

Figure 12: Comparison of the average number of zones and average zone size with different similarities for fixed number of VUEs $K = 20$, $V = 0$, and $N = 15$. The solid lines represent the average number of zones and doted lines represent the average zone size.

resource allocation approach, in which the slow timescale, the RSU groups VUEs in virtual zones leveraging spatial and temporal aspects of network. Subsequently, at each time slot, a matching algorithm is performed to match RBs to VUEs based on their preference list. Finally, using the tools from Lyapunov optimization, every vehicle within specific zone optimizes its transmit power while satisfying queuing latency and reliability constraints. Extensive simulation results have shown that our proposed scheme outperforms a state-of-art baseline and achieves 45% reduction in queuing latency and 94% improvement in terms of reliability.

Appendix A
Proof of Proposition 1

Substituting (4), (9), and (10) into (12), and using $([x]^+)^2 \leq x^2$, we obtain:

$$\begin{aligned}\Delta\big(\boldsymbol{y}(t)\big) \leq \mathbb{E}\Bigg[\sum_{k\in\mathcal{K}}\Big(&\frac{1}{2}q_k(t)^2 + \frac{1}{2}\lambda_k(t)^2 + \frac{1}{2}\tau^2 R_k(t)^2 \\ &+ q_k(t)\lambda_k(t) - \tau q_k(t)R_k(t) - \tau\lambda_k(t)R_k(t) \\ &+ \frac{1}{2}\bar{\lambda}_k^2 d_k^2 - J_k(t)\bar{\lambda}_k d_k \\ &+ J_k(t)\big[q_k(t) + \lambda_k(t) - \tau R_k(t)\big]^+ \\ &- \bar{\lambda}_k d_k\big[q_k(t) + \lambda_k(t) - \tau R_k(t)\big]^+ \\ &+ \frac{1}{2}\mathbb{1}\big\{\big[q_k(t) + \lambda_k(t) - \tau R_k(t)\big]^+ \geq L_k\big\}^2 \\ &+ \frac{1}{2}\epsilon_k^2 + f_k(t)\mathbb{1}\big\{\big[q_k(t) + \lambda_k(t) - \tau R_k(t)\big]^+ \geq L_k\big\} \\ &- f_k(t)\epsilon_k - \epsilon_k\mathbb{1}\big\{\big[Q_k(t) + \lambda_k(t) - \tau R_k(t)\big]^+ \\ &\geq L_k\big\} + \sum_{n\in\mathcal{N}} v p_{kn}(t)\Big)\Big|\boldsymbol{y}(t)\Bigg]. \end{aligned} \tag{34}$$

Then, further applying $\left[q_k(t)+\lambda_k(t)-\tau R_k(t)\right]^+ \leq \max\left\{q_k(t)+\lambda_k(t),\tau R_{k,\max}\right\} - j_k(t)\tau R_k(t)$, we have:

$$\begin{aligned}\Delta\big(\boldsymbol{y}(t)\big) \leq \mathbb{E}\Bigg[\sum_{k\in\mathcal{K}}\Bigg(&\frac{1}{2}q_k(t)^2+\frac{1}{2}\lambda_k(t)^2+\frac{1}{2}^2\tau^2R_{k,\max}^2\\&+q_k(t)\lambda_k(t)+\frac{1}{2}\bar{\lambda}_k^2d_k^2+\frac{1}{2}+\frac{1}{2}\epsilon_k^2\\&+j_k(t)\max\left\{q_k(t)+\lambda_k(t),\tau R_{k,\max}\right\}\\&-\tau q_k(t)R_k(t)-\tau\lambda_k(t)R_k(t)-\tau j_k(t)R_k(t)\\&+f_k(t)\mathbb{1}\left\{\left[Q_k(t)+\lambda_k(t)-\tau R_k(t)\right]^+\geq L_k\right\}\\&+\sum_{n\in\mathcal{N}}vp_{kn}(t)\Bigg)\Big|\boldsymbol{y}(t)\Bigg].\end{aligned} \tag{35}$$

Appendix B
Proof of Lemma 1

Since (32) belongs to a convex optimization problem, we can apply the Karush-Kuhn-Tucker (KKT) conditions to find the optimal solution. Subsequently, applying the KKT conditions, the optimal solution $P_{kn}^*, \forall\, n\in\mathcal{N}_k$, satisfies:

$$\begin{cases}\dfrac{\tau\big(j_k+f_k+2q_k+2\lambda_k\big)}{\ln 2}\\ \quad\times\mathbb{E}_{I_{kn}}[\Psi]=v+\gamma-\gamma_{kn},\ \forall\, n\in\mathcal{N}_k, & \text{(36a)}\\ p_{kn}^*\geq 0,\ \forall\, n\in\mathcal{N}_k, & \text{(36b)}\\ \gamma_{kn}\geq 0,\ \forall\, n\in\mathcal{N}_k, & \text{(36c)}\\ p_{kn}^*\gamma_{kn}=0,\ \forall\, n\in\mathcal{N}_k, & \text{(36d)}\\ \displaystyle\sum_{n\in\mathcal{N}_z}p_{kn}^*\leq P_k^{\max}, & \text{(36e)}\\ \gamma\geq 0, & \text{(36f)}\\ \gamma\Big(\displaystyle\sum_{n\in\mathcal{N}_z}p_{kn}^*-P_k^{\max}\Big)=0, & \text{(36g)}\end{cases}$$

with $\Psi=\frac{p_{kn}^*}{\sigma^2+I_{kn}+p_{kn}^*|h_{kkn}|^2}$. In addition, γ and $\gamma_{kn},\forall\, n\in\mathcal{N}_k$ are the Lagrange multipliers. From (36a)–(36d), we can deduce that if $\frac{\tau\omega\left(j_k+f_k+2q_k+2\lambda_k\right)}{\ln 2}\times\mathbb{E}\Big[\frac{h_{kkn}}{\sigma^2+I_{kn}^{\text{inter-zone}}}\Big] > v+\gamma,\forall\, n\in\mathcal{N}_z$, the VUE allocates a positive transmit power $p_{kn}^*>0$ over RB n which satisfies

$$\frac{\tau\big(j_k+f_k+2q_k+2\lambda_k\big)}{\ln 2}\times\mathbb{E}\left[\frac{h_{kkn}}{\sigma^2+I_{kn}^{\text{inter-zone}}+p_{kn}^*h_{kkn}}\right] = v+\gamma. \tag{37}$$

Otherwise, $p_{kn}^*=0$. According to (36e)–(36g), we let the Lagrange multiplier $\gamma=0$ if $\sum_{n\in\mathcal{N}_k}p_{kn}^*<P_k^{\max}$, and $\sum_{n\in\mathcal{N}_k}p_{kn}^*=P_k^{\max}$ when $\gamma>0$.

References

[1] G. Araniti, C. Campolo, M. Condoluci, A. Iera, and A. Molinaro, "LTE for vehicular networking: A survey," *IEEE Commun. Mag.*, vol. 51, no. 5, pp. 148–157, May 2013.

[2] "ETSI EN Std 302 637-2, Intelligent transport systems; Vehicular communications; Basic set of applications; Part 2: Specification of cooperative awareness basic service, v. 1.3.0," Aug. 2013.

[3] "ETSI EN Std 302 637-3, Intelligent transport systems; Vehicular communications; basic set of applications; Part 3: Specification of decentralized environmental notification basic service, v. 1.2.0," Aug. 2013.

[4] C. Lottermann, M. Botsov, P. Fertl, R. Müllner, G. Araniti, C. Campolo, M. Condoluci, A. Iera, and A. Molinaro, *LTE for Vehicular Communications*. Springer International Publishing, 2015, pp. 457–501.

[5] A. Osseiran, F. Boccardi, V. Braun, K. Kusume, P. Marsch, M. Maternia, O. Queseth, M. Schellmann, H. Schotten, H. Taoka, H. Tullberg, M. A. Uusitalo, B. Timus, and M. Fallgren, "Scenarios for 5G mobile and wireless communications: The vision of the METIS project," *IEEE Commun. Mag.*, vol. 52, no. 5, pp. 26–35, May 2014.

[6] 3GPP TR 38.913, "3GPP, Study on scenarios and Requirements for Next Generation Access Technologies, Technical Specification Group Radio Access Network, Release 14," Oct. 2016.

[7] M. Bennis, M. Debbah, and H. V. Poor, "Low-latency wireless communication: Tail, risk and scale," *Proc. of the IEEE, submitted*, 2018, [Online]. Available:https://arxiv.org/pdf/1801.01270.

[8] "Nokia, 5G highlights, 5G Technology Workshop - Potential Technology for 3GPP Rel-15," Oct. 2016, [Online]. Available:https://www.slideshare.net/eikoseidel/nokia-5g-workshop-taiwan-oct-2016.

[9] A. Vinel, "3GPP LTE versus IEEE 802.11p/WAVE: Which technology is able to support cooperative vehicular safety applications?" *IEEE Wireless Commun. Lett.*, vol. 1, no. 2, pp. 125–128, Apr. 2012.

[10] X. Cheng, L. Yang, and X. Shen, "D2D for intelligent transportation systems: A feasibility study," *IEEE Trans. Intell. Transp. Syst.*, vol. 16, no. 4, pp. 1784–1793, Aug. 2015.

[11] W. Sun, E. G. Ström, F. Brännström, K. C. Sou, and Y. Sui, "Radio resource management for D2D-based V2V communication," *IEEE Trans. Veh. Technol.*, vol. 65, no. 8, pp. 6636–6650, Aug. 2016.

[12] M. Botsov, M. Klügel, W. Kellerer, and P. Fertl, "Location dependent resource allocation for mobile device-to-device communications," in *Proc. of IEEE Wireless Commun. Netw. Conf.*, Apr. 2014, pp. 1679–1684.

[13] S. Zhang, Y. Hou, X. Xu, and X. Tao, "Resource allocation in D2D-based V2V communication for maximizing the number of concurrent transmissions," in *Proc. of IEEE 27th Annu. Int. Symp. Pers., Indoor, Mobile Radio Commun.*, Sep. 2016, pp. 1–6.

[14] B. Bai, W. Chen, K. B. Letaief, and Z. Cao, "Low complexity outage optimal distributed channel allocation for vehicle-to-vehicle communications," *IEEE J. Sel. Areas Commun.*, vol. 29, no. 1, pp. 161–172, Jan. 2011.

[15] L. Liang, G. Li, and W. Xu, "Resource allocation for D2D-enabled vehicular communications," *IEEE Trans. Commun.*, 2017, to be published.

[16] W. Xing, N. Wang, C. Wang, F. Liu, and Y. Ji, "Resource allocation schemes for D2D communication used in VANETs," in *Proc. of IEEE 80th Veh. Technol. Conf.*, Sep. 2014, pp. 1–6.

[17] M. I. Ashraf, M. Bennis, C. Perfecto, and W. Saad, "Dynamic proximity-aware resource allocation in vehicle-to-vehicle (V2V) communications," in *Proc. of IEEE Global Commun. Conf. Workshops*, Dec. 2016, pp. 1–6.

[18] Y. Ren, C. Wang, D. Liu, F. Liu, and E. Liu, "Applying LTE-D2D to support V2V communication using local geographic knowledge," in *Proc. of IEEE 82nd Veh. Technol. Conf.*, Sep. 2015, pp. 1–5.

[19] M. Wilhelm, T. Higuchi, and O. Altintas, "Geo-spatial resource allocation for heterogeneous vehicular communications: Poster," in *Proc. of 17th ACM Int. Symp. Mobile Ad Hoc Netw. Comput.*, Jul. 2016, pp. 399–400.

[20] M. I. Ashraf, C.-F. Liu, M. Bennis, and W. Saad, "Towards low-latency and ultra-reliable vehicle-to-vehicle communication," in *2017 European Conference on Networks and Communications (EuCNC)*, June 2017, pp. 1–5.

[21] C. She, C. Yang, and T. Q. S. Quek, "Radio resource management for ultra-reliable and low-latency communications," *IEEE Communications Magazine*, vol. 55, no. 6, pp. 72–78, 2017.

[22] M. Mozaffari, W. Saad, M. Bennis, and M. Debbah, "Unmanned aerial vehicle with underlaid device-to-device communications: Performance and tradeoffs," *IEEE Transactions on Wireless Communications*, vol. 15, no. 6, pp. 3949–3963, June 2016.

[23] O. Semiari, W. Saad, S. Valentin, M. Bennis, and H. V. Poor, "Context-aware small cell networks: How social metrics improve wireless resource allocation," *IEEE Transactions on Wireless Communications*, vol. 14, no. 11, pp. 5927–5940, Nov 2015.

[24] T. Zeng, O. Semiari, W. Saad, and M. Bennis, "Joint communication and control for wireless autonomous vehicular platoon systems," 04 2018, [Online]. Available:https://arxiv.org/pdf/1804.05290.

[25] M. J. Neely, *Stochastic Network Optimization with Application to Communication and Queueing Systems*. Morgan and Claypool Publishers, Jun. 2010.

[26] J. D. C. Little, "A proof for the queuing formula: $L=\lambda W$," *Operations Research*, vol. 9, no. 3, pp. 383–387, 1961.

[27] A. T. Z. Kasgari and W. Saad, "Stochastic optimization and control framework for 5g network slicing with effective isolation," in *Proc. of 52nd Annual Conference on Information Sciences and Systems (CISS)*, March 2018, pp. 1–6.

[28] M. J. Neely, "Energy optimal control for time-varying wireless networks," *IEEE Transactions on Information Theory*, vol. 52, no. 7, pp. 2915–2934, July 2006.

[29] ——, "A Lyapunov optimization approach to repeated stochastic games," in *Proc. of 51st Annual Allerton Conference on Communication, Control, and Computing, Monticello, IL, USA, October 2-4, 2013*, 2013, pp. 1082–1089.

[30] K. Seong, M. Mohseni, and J. M. Cioffi, "Optimal resource allocation for OFDMA downlink systems," in *Proc. of IEEE Int. Symp. Inf. Theory*, Jul. 2006, pp. 1394–1398.

[31] U. Luxburg, "A tutorial on spectral clustering," *Statistics and Computing*, vol. 17, no. 4, pp. 395–416, Dec. 2007. [Online]. Available: http://dx.doi.org/10.1007/s11222-007-9033-z

[32] A. E. Roth and M. A. O. Sotomayor, *Two-Sided Matching: A Study in Game-Theoretic Modeling and Analysis*. Cambridge University Press, 1992.

[33] Y. Gu, W. Saad, M. Bennis, M. Debbah, and Z. Han, "Matching theory for future wireless networks: Fundamentals and applications," *IEEE Commun. Mag.*, vol. 53, no. 5, pp. 52–59, May 2015.

[34] S. Bayat, Y. Li, L. Song, and Z. Han, "Matching theory: Applications in wireless communications," *IEEE Signal Process. Mag.*, vol. 33, no. 6, pp. 103–122, Nov. 2016.

[35] E. A. Jorswieck, "Stable matchings for resource allocation in wireless networks," in *Proc. of 17th Int. Conf. Digit. Signal Process.*, Jul. 2011, pp. 1–8.

[36] D. Gale and L. S. Shapley, "College admissions and the stability of marriage," *Cambridge University Press, Cambridge*, vol. 69, no. 1, pp. 9–15, 1992.

[37] P. Heino, E. Suikkanen, E. Kunnari, J. Meinilä, P. Kyösti, L. Hentilä, T. Jämsä, and M. Narandžić, "D5.3: WINNER + final channel models," p. 107, 2010.

[38] 3GPP TR 38.885, "Study on scenarios and Requirements for Next Generation Access Technologies, Technical Specification Group Radio Access Network, Study on LTE-based V2X Services, Release 14," Feb. 2016.

[39] G. W. RP-161894, "Initial cellular V2X standard," Sep. 2016.

[40] M. Molina, O. Muñoz, A. Pascual-Iserte, and J. Vidal, "Joint scheduling of communication and computation resources in multiuser wireless application offloading," in *Proc. of IEEE 25th Annu. Int. Symp. Pers., Indoor, Mobile Radio Commun.*, Sep. 2014, pp. 1093–1098.